Available online at www.sciencedirect.com
SCIENCE DIRECT
Clinical Biomechanics 21 (2006) 710–716
CLINICAL BIOMECHANICS
www.elsevier.com/locate/clinbiomech

An identification technique for evaluating body segment parameters in the upper extremity from manipulator-hand contact forces and arm kinematics

Timotej Kodek *, Marko Munih

University of Ljubljana, Faculty of Electrical Engineering, Laboratory of Robotics and Biomedical Engineering, Tržaška 25, 1000 Ljubljana, Slovenia

Received 5 August 2005; accepted 17 February 2006

Abstract

Objective. To show that it is possible to determine segment masses and segment centers of mass by measuring manipulator-hand contact forces and joint angles during upper extremity movement.

Background. The method serves as a quick subject specific body segment parameter evaluation technique. Clinically we see this method as an alternative upper extremity body segment parameter evaluation study especially useful in rehabilitation treatment activities.

Methods. The experiment is based on coupling the human arm with a robotic manipulator which is then used for imposing a specified sagittal plane trajectory. Joint angles and forces in the contact point serve as input to the identification procedure. For verification purposes the proposed identification procedure was first performed on a mechanical arm. Afterwards a low velocity trajectory was imposed into all joints of the human upper extremity, with very small angular deviations. Within this small angular region the arm was assumed to be represented as a linear system.

Findings. The outcome of the identification procedure is an estimate of masses and center of mass coordinates for the lower arm and palm segments, their products for the upper arm and the passive moments around the measured angle of all joints in the sagittal plane. The results obtained for three particular human arms are eventually compared to the average population based literature.

Conclusion. From the clinical point of view the study can become useful for biomechanical evaluation and for evaluating biomechanical properties of lower extremities or other body segments. This method may also provide a foundation to measuring body segment moments of inertia and joint viscoelastic parameters.

Keywords: Segment mass; Segment center of mass; Upper extremity; Identification; Body segment parameter

1. Introduction

In many of today's biomechanical studies there is a need for estimating body segment parameters (BSP) such as masses, centers of mass (COM) and inertial moments. These parameters are often required for modelling purposes as well as in studies which evaluate performances in fields such as rehabilitation engineering or kinesiological studies (van de Hel et al., 2001; Hinrichs, 1985). Due to obvious difficulties in determining these data for a particular person directly, authors usually refer to studies from the literature. These state the desired parameters in the form of regression curves as a function of easily measurable quantities such as body masses and body heights. The oldest studies were made in vitro on cadavers and only dealt with a relatively small test group. The importance of such data is indicated by the fact that the oldest comprehensive study was already made in 1860 by Harless (1860). The most comprehensive study including 152 living male and female

* Corresponding author.
E-mail address: timotej.kodek@robo.fe.uni-lj.si (T. Kodek).

0268-0033/$ - see front matter © 2006 Elsevier Ltd. All rights reserved.
doi:10.1016/j.clinbiomech.2006.02.006

subjects was performed by Bernstein (1947) utilizing the method of reaction change where the subjects body segment COMs were measured in different configurations while lying on a balance plate. Recently similar methodology was used and put into context with other literature studies by Pataky et al. (2003) who performed an analysis of body segment masses on a group of 35 young athletes. Among the still commonly cited in vitro studies are the pioneering works of Dempster (1955) and Clauser et al. (1969). The former analyzed 8 male cadavers with an average age of 68.5 years, while the latter focused on a group of 13 male cadavers with an average age of 49.3 years. Today most such studies are non-invasive, performed in vivo involving a larger number of subjects. Among these a well known study was made by Zatsiorsky and Seluyanov (1983) who used the γ-ray absorbtion method for measuring average segment densities on a large group of 100 healthy young Caucasian male subjects. Data coming from a slight modification of geometrical body segment coordinates in this method, performed by de Leva (1995), is often used in many present day biomechanical studies.

With technological progress in the last decades some other non-invasive methods have also become available. The most significant ones are Computer Tomography and Magnetic Resonance Imaging, which both give detailed information concerning the distribution of internal structures including tissues and bones in body segments. By assuming the mean tissue density values and accounting for the measured spatial distributions, it is then possible to calculate the values of various BSPs. Several attempts in this direction have already been made (Wei and Jensen, 1995; Martin et al., 1989; Mungiole and Martin, 1990; Reynolds and Walt, 2002). Out of these only the study of Wei and Jensen (1995) was performed on a larger group consisting of 50 individuals. Others, however, do not give a comprehensive analysis on a large test group of individuals, but it must be said that both methods offer good prospects for future research.

Considering all these studies a question of estimated regression curve accuracies arises. The body segment properties among various people may differ quite significantly due to factors such as different body structure, age or gender. For example, the average age of subjects involved in the study of Zatsiorsky and Seluyanov (1983) was approximately 24 years, whereas many of today's studies requiring BSPs focus on older individuals who have in the past suffered from certain neuromuscular disorders. Unsurprisingly, Hinrichs (1985) stated: "The use of indirect estimates of body segment masses, centers of mass and moments of inertia is arguably one of the biggest sources of error in biomechanics research."

Following the problem addressed above our study proposes an alternative in vivo technique for determining values of some significant BSPs in the upper extremity by utilizing an optimization curve fitting technique. In the presented experimental work, parameters were first estimated on a mechanical arm to obtain the accuracy level of the procedure. Afterwards the same process was performed on upper extremities of three healthy young male individuals. The obtained data is then presented and compared to literature studies.

2. Methods

The experiment is based on moving the upper extremity along a specified trajectory with a robotic manipulator (Fig. 1). The trajectory was chosen in a way which imposed very slow (quasi-static) angular deviations into all joints (Fig. 4). During this process joint angle data was collected by means of an infrared marker based motion tracking system (*Optotrak© – NDI International, Ontario, Canada*), as well as forces in the contact point. Collection frequencies in both cases were 50 Hz. An approval of the Slovenian medical ethics commission was obtained prior to the experiment. Ten measurements (acquired in one single trial on one day) were performed on the left arm of three healthy young male individuals.

The manipulator-hand contact forces and moments $F_e = [F_y, F_z, M_x]^{\mathrm{T}}$ were measured with a strain gauge force sensor. (*JR3© – JR3 Inc., Woodland, CA, USA*) Due to a bearing at the robot attached handle, the torque value M_x was minimal.

The human arm was simplified as a 3DOF rigid body planar structure in the sagittal plane with the following notation (Fig. 2).

The segment lengths are denoted with a_j, their COM lengths from the proximal joint with l_j while q_j indicates joint angle directions with respect to the zero position (dashed line). The shoulder zero angle position was chosen horizontally. The segment masses are presented with m_j.

The inverse dynamics of the human arm can be described as a relationship between the applied muscle produced torques $\boldsymbol{\tau}(\mathbf{u})$, environment joint contributions $\boldsymbol{\tau}_{\mathrm{end}}$ and the joint motion trajectory of mechanical joints (Siciliano and Sciavicco, 1996):

$$\boldsymbol{\tau}_B(\ddot{\mathbf{q}}) + \boldsymbol{\tau}_{\mathrm{C}}(\mathbf{q}, \dot{\mathbf{q}}) + \boldsymbol{\tau}_{\mathrm{G}}(\mathbf{q}) + \boldsymbol{\tau}_{\mathrm{vel}}(\dot{\mathbf{q}}, \mathbf{q}, \mathbf{u}) + \boldsymbol{\tau}_{\mathrm{d}}(\mathrm{sgn}(\dot{\mathbf{q}}), \mathbf{q}, \mathbf{u}) = \boldsymbol{\tau}(\mathbf{u}) - \boldsymbol{\tau}_{\mathrm{end}}. \quad (1)$$

Every one of the terms in Eq. (1) represents a three-dimensional torque vector with the shoulder as first, elbow as second and wrist as the third coordinate. $\boldsymbol{\tau}_B(\ddot{\mathbf{q}})$ represents *inertial contributions*, $\boldsymbol{\tau}_{\mathrm{C}}(\mathbf{q}, \dot{\mathbf{q}})$ the *centrifugal – Coriolis* contributions and $\boldsymbol{\tau}_{\mathrm{G}}(\mathbf{q})$ the gravity effects on the arm dynamics. The viscoelastic moments $\boldsymbol{\tau}_{\mathrm{vel}}(\dot{\mathbf{q}}, \mathbf{q}, \mathbf{u})$ arise in every joint as a consequence of various structures (e.g. tendons, ligaments, muscles). They are a non-linear function of adjacent joint angles and muscle activation u (Hatze, 1997; Esteki and Mansour, 1996; Riener and Edrich, 1999; Kodek and Munih, 2003; Mansour and Audu, 1986). The dissipative torques $\boldsymbol{\tau}_{\mathrm{d}}(\mathrm{sgn}(\dot{\mathbf{q}}), \mathbf{q}, \mathbf{u})$ represent the direction dependent Coulomb friction components. On the right side of Eq. (1) there are active muscle contributions $\boldsymbol{\tau}(\mathbf{u})$ and torques caused by the environment $\boldsymbol{\tau}_{\mathrm{end}}$.

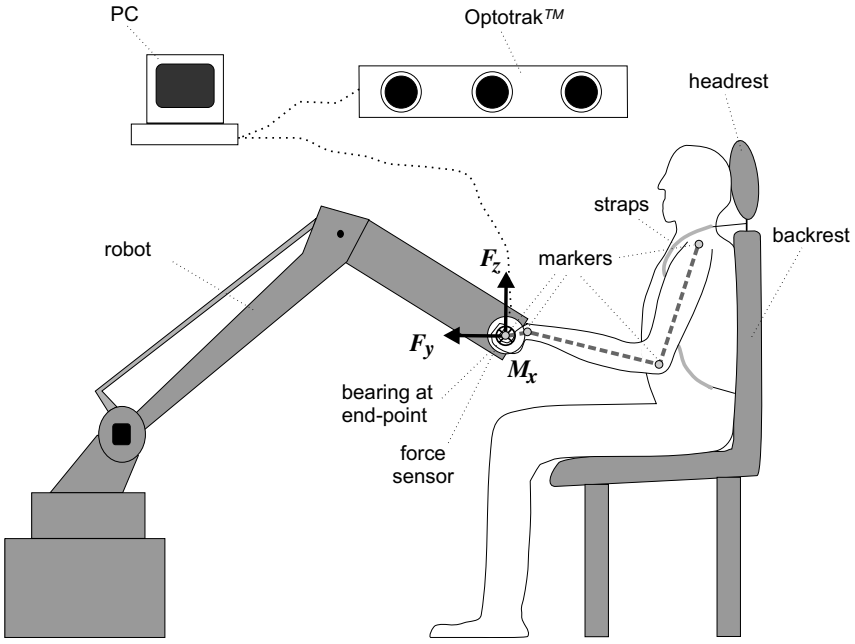

Fig. 1. A side view of the experimental setup. The subject is seated on a strap equipped passenger type seat which minimizes trunk movements. Four infrared markers were attached at joint rotation centers as recommended in de Leva (1995).

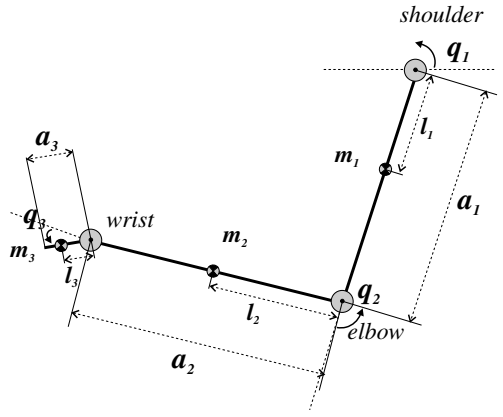

Fig. 2. Geometric definitions for the assumed human arm structure, consisting of three rigid body segments.

Kinematic variables $\mathbf{q}$, $\dot{\mathbf{q}}$ and $\ddot{\mathbf{q}}$ represent the angle, angular velocity and angular acceleration transpose vectors. Joint angles were obtained from acquired marker spatial data while the angular velocity and accelerations were a result of numerical derivation. All kinematic data was also low-pass filtered at 5 Hz.

Our experimental analysis was done under two fundamental assumptions:

(1) All performed movements were *very slow* with angular velocities around 0.03 rad/s. After observing the very small contributions of dynamic terms in Eq. (1) under these conditions we have assumed that the experiment was always performed under quasi-static conditions.

(2) We decided to perform all experimental movements with the upper *extremity muscles in a relaxed condition*. To exclude muscle activity due to gripping the arm was lightly strapped to the robot. To prove that the subject induced no voluntary action during the course of the experiment we have observed the EMG signals of four muscles in a typical elbow flexion–extension movement prior to doing any experimental work (*i.e. biceps long head, biceps short head, triceps* and *brachioradialis*). The EMG signals showed practically no muscular activity at all.

On the basis of these two assumptions we made the following simplifications:

$$\boldsymbol{\tau}_B = \mathbf{0}, \quad \boldsymbol{\tau}_C = \mathbf{0}, \quad \tau(\mathbf{u}) = 0. \tag{2}$$

By accounting for all these, the simplified version of Eq. (1) can now be written as

$$\boldsymbol{\tau}_G(\mathbf{q}) + \boldsymbol{\tau}_p(\mathbf{q}) = -\boldsymbol{\tau}_{end} = -\mathbf{J}^T(\mathbf{q})\mathbf{F}_{end}. \tag{3}$$

Gravity vector $\boldsymbol{\tau}_G(\mathbf{q})$ joint torque components can now be expressed as

$$\begin{aligned} \tau_{g1} &= g_0\{[l_1m_1 + a_1(m_2 + m_3)]c_1 \\ &\quad + (l_2m_2 + a_2m_3)c_{12} + l_3m_3c_{123}\}, \\ \tau_{g2} &= g_0[(l_2m_2 + a_2m_3)c_{12} + l_3m_3c_{123}], \\ \tau_{g3} &= g_0l_3m_3c_{123}. \end{aligned} \tag{4}$$

τ_{g1} stands for gravity shoulder joint contribution, τ_{g2} for the gravity elbow joint contribution and τ_{g3} for gravity wrist joint contribution. Please note that the following notation was used: $c_1 = \cos(q_1)$, $c_{12} = \cos(q_1 + q_2)$, $c_{123} = \cos(q_1 + q_2 + q_3)$. g_0 represents the gravity constant.

In Eq. (3), $\boldsymbol{\tau}_{\text{vel}}$ has been replaced with the passive moments term $\boldsymbol{\tau}_{\text{p}}(\mathbf{q})$. These passive moments are no longer velocity and muscle activation dependent but rather a *non-linear function* of only the adjacent joint angles. By definition these torques include elastic and direction dependent dissipative components and arise mostly due to passive muscles surrounding joints (Mansour and Audu, 1986; Riener and Edrich, 1999). The environment contributions $\boldsymbol{\tau}_{\text{end}}$ are obtained by premultiplication of the manipulator-hand contact force vector $\mathbf{F}_{\text{end}} = [\mathbf{F}_y, \mathbf{F}_z, \mathbf{M}_x]^{\text{T}}$ with a Jacobian matrix of a 3DOF planar manipulator $\mathbf{J}^{\text{T}}(\mathbf{q})\mathbf{F}_{\text{end}}$ (Siciliano and Sciavicco, 1996).

2.1. Parameter identification procedure

Because angular deviations in all joints were small in all measurements ($\Delta|q_j| < 12°$) no large non-linearities have been observed. We therefore concluded that the $\boldsymbol{\tau}_{\text{p}}$ non-linearities were small enough to allow an assumption of system linearity within this angular region. Following this we can now express Eq. (3) as the following linear relationship (An et al., 1988):

$$\mathbf{Y}_j\boldsymbol{\pi}_j = \boldsymbol{\tau}_j, \text{ at time } t_i \tag{5}$$

$\mathbf{Y}_j$ represents the regression vector for segment j, with which we should multiply the corresponding vector of identification parameters $\boldsymbol{\pi}_j$ to obtain τ_j which represents all remaining known terms.

Let us now present the system in Eq. (5) with three consecutive linear equations, describing the inverse dynamics of every particular joint at time t_i:

- *Wrist joint:*

$$g_0\cos_{123}m_3l_3 + \tau_{p3} = \tau_{\text{end}3}$$

or in matrix form,

$$\mathbf{Y}_3\boldsymbol{\pi}_3 = [\,g_0\cos_{123}, \quad 1\,][\,m_3l_3, \quad \tau_{p3}\,]^{\text{T}} = \boldsymbol{\tau}_3. \tag{6}$$

By accounting for m_3l_3 obtained from the wrist identification vector π_3 the elbow equation can now be written.

- *Elbow joint:*

$$g_0\cos_{12}m_2l_2 + g_0a_2\cos_{12}m_3 + \tau_{p2} = \tau_{e2} - g_0\cos_{12}m_3l_3$$

or in matrix form,

$$\mathbf{Y}_2\boldsymbol{\pi}_2 = [\,g_0\cos_{12}, \quad g_0a_2\cos_{12}, \quad 1\,][\,m_2l_2, \quad m_3, \quad \tau_{p2}\,]^{\text{T}} = \tau_2. \tag{7}$$

By accounting for m_3l_3 obtained in step 1, m_2l_2 and m_3 from π_2 we can now write the shoulder joint equation (Eq. (8)).

- *Shoulder joint:*

$$g_0\cos_1m_1l_1 + g_0a_1\cos_1m_2 + \tau_{p1} = \tau_{e1} - g_0(a_1\cos_1 + a_2\cos_{12})m_3 - g_0\cos_{12}m_2l_2 - g_0\cos_{123}m_3l_3$$

or in matrix form,

$$\mathbf{Y}_1\boldsymbol{\pi}_1 = [\,g_0\cos_1, \quad g_0a_1\cos_1, \quad 1\,][\,m_1l_1, \quad m_2, \quad \tau_{p1}\,]^{\text{T}} = \tau_1. \tag{8}$$

From all three joint equations it can be deduced that the identification vectors π_j were chosen as $\pi_3 = [m_3l_3, \tau_{p3}]^{\text{T}}$, $\pi_2 = [m_2l_2, m_3, \tau_{p2}]^{\text{T}}$ and $\pi_3 = [m_1l_1, m_2, \tau_{p1}]^{\text{T}}$. By considering Eqs. (7) and (8), we can see that solving for every particular $\boldsymbol{\pi}_j$ at N time instants t_i represents a linearly dependent problem since a_2 and a_1 are constants representing lower and upper arm lengths. Therefore the problem of identifying vectors π_j is described as an optimization problem, which minimizes the difference between both sides of Eq. (5). At t_i, this difference can be expressed as the following function:

$$F_{t_i}(\boldsymbol{\pi}_j) = \boldsymbol{\tau}_j - \mathbf{Y}_j\boldsymbol{\pi}_j. \tag{9}$$

The algorithm calculates π_j as a result of a *constrained non-linear least squares optimization* for all time samples $1 \leqslant t_i \leqslant N$ using the Matlab™ `lsqnonlin` function which solves the following minimization (Lawson and Hanson, 1974):

$$\min_{\boldsymbol{\pi}_j} \sum_{t_i=1}^{N} F_{t_i}(\boldsymbol{\pi}_j)^2, \text{ such that } \text{lb} \leqslant \boldsymbol{\pi}_j \leqslant \text{ub}. \tag{10}$$

The constraints lb and ub were chosen suitably for every particular identification vector. It needs to be pointed out that the algorithm was very insensitive to the value of these limits.

2.2. Algorithm verification with a mechanical model

To verify the accuracy of the described algorithm, a preliminary experiment was conducted using a CAD designed 2DOF mechanical arm. The segment lengths and masses of the model were chosen comparably to the human arm (Fig. 3). To simulate joint passive moments, screw-adjustable rubber brakes were attached at every joint. These brakes produced a desirable Coulomb friction force by pressing on stainless steel disks from both sides. The level of the friction was arbitrarily chosen to have a significant value. The friction force was directly measured with a load cell mounted at a 45° angle, enabling the computation of brake-produced passive moments as seen from Fig. 3.

The mechanical arm was coupled with the robot by using a screw attached to a bearing. The motion trajectories and manipulator-hand contact forces were measured in the same way as with a human subject.

The identification procedure we used, was the same as the one described previously, the only difference being the number of identification parameters. Since the model now only consisted of two segments (upper and lower arm), only two identification vectors $\boldsymbol{\pi}_{jR}$ had to be determined, consisting of a total number of five identification parameters: ($\boldsymbol{\pi}_{2R} = [m_{2R}l_{2R}, \tau_{p2R}]^{\text{T}}$ and $\boldsymbol{\pi}_{1R} = [m_{1R}l_{1R}, m_{2R}, \tau_{p1R}]^{\text{T}}$).

The imposed trajectory was a flexion–extension movement as seen in Fig. 4.

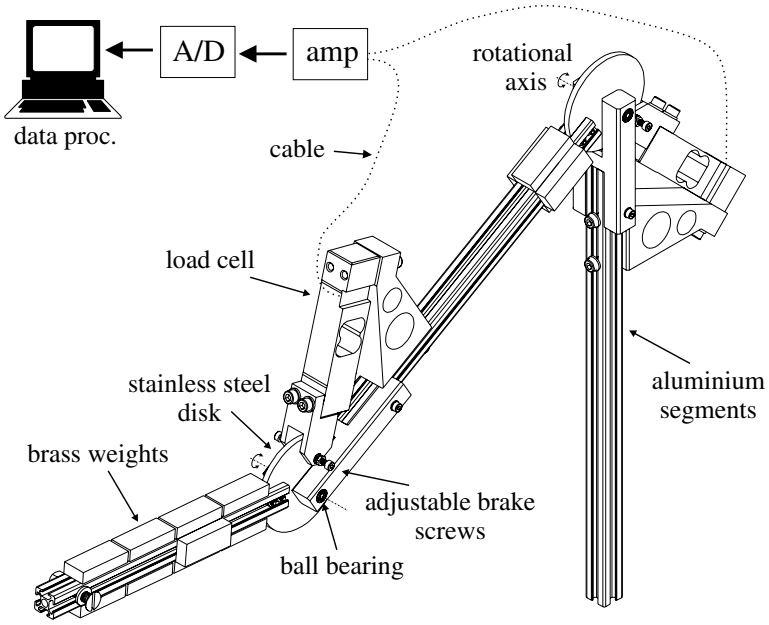

Fig. 3. The 2DOF mechanical model used for algorithm verification. Two HBM type PW2FC3 one dimensional aluminium strain gage load cells were used for measuring mechanical friction. To obtain masses comparable to the human arm, brass weights were properly attached to the aluminium segments. The load cell signals were amplified, digitalized and processed together with manipulator-hand contact forces and Optotrak© motion data.

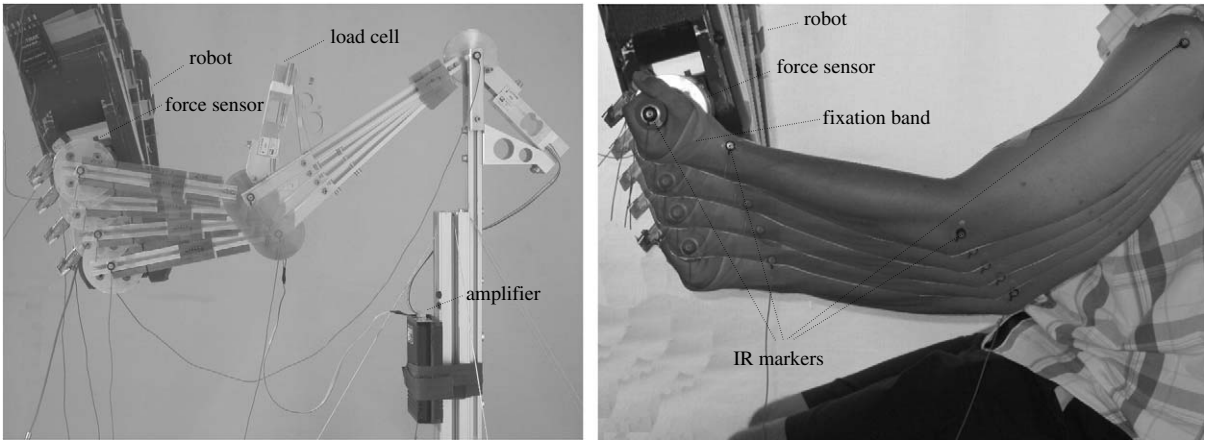

Fig. 4. Two composite images showing the complete courses of the mechanical arm trajectory with shoulder and elbow angular ranges of ±5.7° around $\bar{q}_1 = -36.6°$ and ±5.7° around $\bar{q}_2 = 35.8°$ respectively (left). The trajectory of the human arm (right) during the measurement with shoulder, elbow and wrist angular ranges of ±6° around $\bar{q}_1 = -43.3°$, ±1.7° around $\bar{q}_2 = 29.5°$ and ±0.9° around $\bar{q}_3 = 0.2°$ respectively.

The best optimization results were obtained when the upper and lower optimization bounds (ub and lb in Eq. (10)) for passive moments τ_{pjR} were initially set to values around zero as $\boldsymbol{\pi}_{2R} = [m_{2R}l_{2R}, 0]^{\mathrm{T}}$ and $\boldsymbol{\pi}_{1R} = [m_{1R}l_{1R}, m_{2R}, 0]^{\mathrm{T}}$.

Fig. 5 gives an insight into the horizontal and vertical manipulator-hand contact force trajectories (left) and into identified joint torques (right) of the mechanical model. The identified joint torque τ_{jR} is represented with the central continuous trajectory in the cases of both joints. This trajectory clearly shows that the direction dependent τ_{p1} and τ_{p2} visible in the measured torques were not accounted for. The measured torques obtained from the force and kinematic data was denoted with $\tau_{j\mathrm{meas}R}$ with the Coulomb friction components clearly visible.

The passive moment value τ_{pjR} was now obtained by observing the absolute difference between all time samples of the identified joint torque trajectory $\tau_{jR} = \mathbf{Y}_{jR}\boldsymbol{\pi}_{jR}$ and the corresponding measured trajectory $\tau_{j\mathrm{meas}R}$ as

$$\tau_{pjR} = \frac{1}{N}\sum_{i=1}^{N} |\tau_{\mathrm{jmeas}R}(t_i) - \tau_{jR}(t_i)|. \tag{11}$$

The same procedure was also used when determining passive moments in the human arm joints. The joint passive moments τ_{pj} were hence also presumed to consist only of direction dependent dissipative contributions (Mansour and Audu, 1986; Riener and Edrich, 1999), while the elastic components were confirmed to lie around zero in the measured angular region by a previous study (Kodek and Munih, 2003).

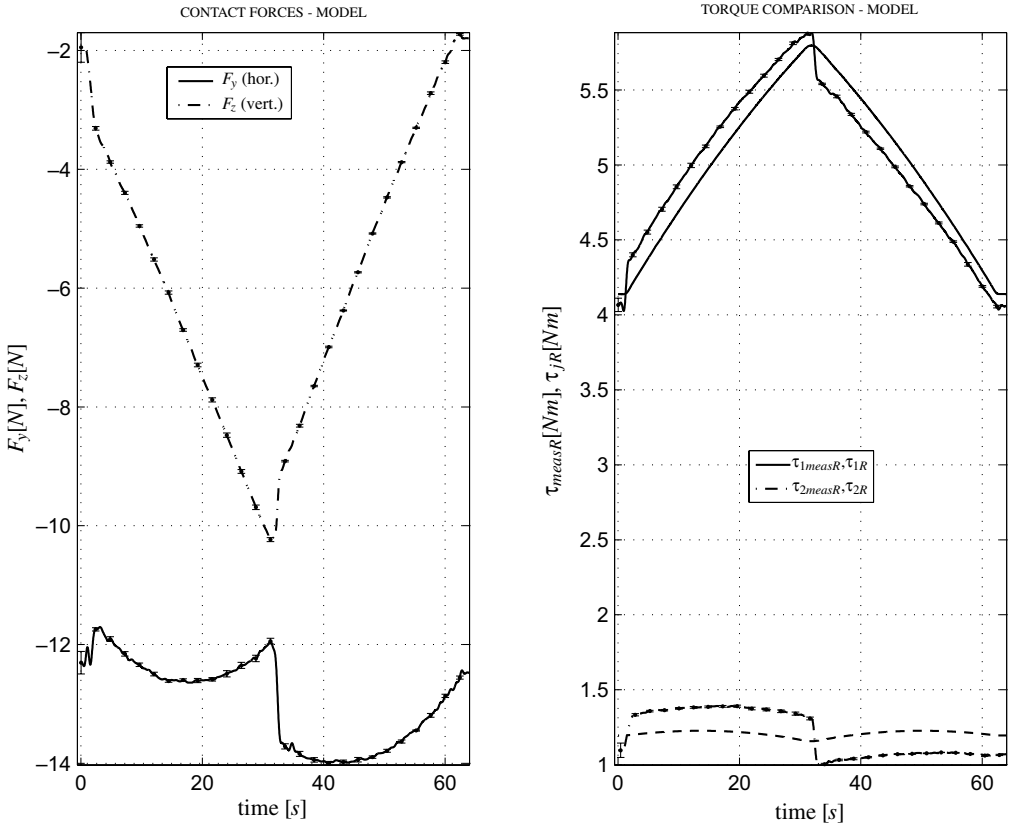

Fig. 5. Ten measurement average horizontal (F_y) and vertical (F_z) manipulator-hand contact forces with measurement standard deviations shown for the mechanical model (left). The right figure gives a comparison between the measured joint torques τ_{jmeasR} and the corresponding identified torques τ_{jR}.

3. Results

The numerical results for segment parameter identification are summarized separately for the mechanical arm (Table 1 – upper part) and for the human arm (Table 1 – lower part). In the mechanical arm the variable x_{ref} denotes the CAD obtained parameters values, while in the human arm this variable denotes literature obtained estimates (Zatsiorsky and Seluyanov, 1983). The identified parameter values are represented with $\bar{x}$ as average values from 10 measurements. The 10 measurement standard deviations (σ_x) and differences in relative form $\left(\frac{x_{ref}-\bar{x}}{\bar{x}}\right)$ are also given in both parts of the table. Reference values of passive moment parameters τ_{pj} are not given for the human subject because they are very subject specific (Kodek and Munih, 2003) and as such not available in literature studies.

Table 1
Significant parameters obtained for the mechanical arm

Parameter	x_{ref}	$\bar{x}$	σ_x	$\frac{\lvert\bar{x}-x_{ref}\rvert}{x_{ref}}(\%)$
$m_{2R}l_{2R}$ (kgm)	0.130	**0.125**	0.001	3.8
m_{2R} (kg)	1.160	**1.206**	0.001	3.9
l_{2R} (m)	0.115	**0.104**	0.001	9.8
$m_{1R}l_{1R}$ (kgm)	0.260	**0.265**	0.001	1.8
τ_{p2R} (Nm)	0.161	**0.145**	0.006	7.7
τ_{p1R} (Nm)	0.139	**0.151**	0.007	10.6
m_3l_3 (kgm)	0.047	**0.088**	0.002	89, (127, 95)
m_3 (kg)	0.663	**0.719**	0.002	8, (24, 7)
l_3 (m)	0.070	**0.123**	0.004	74, (83, 82)
m_2l_2 (kgm)	0.154	**0.122**	0.015	21, (10, 18)
m_2 (kg)	1.247	**1.256**	0.004	1, (9, 29)
l_2 (m)	0.124	**0.097**	0.011	21, (1, 16)
m_1l_1 (kgm)	0.393	**0.406**	0.003	3, (43, 58)
τ_{p3} (Nm)	/	**0.062**	0.014	/
τ_{p2} (Nm)	/	**0.277**	0.014	/
τ_{p1} (Nm)	/	**0.513**	0.003	/

$\bar{x}$ denotes the average values from 10 measurements. Measurement standard deviations are denoted as σ_x and differences in relative form as $\frac{\lvert\bar{x}-x_{ref}\rvert}{x_{ref}}$. The numbers in brackets in the lower table part give an insight into errors obtained for the second and third subjects.

4. Discussion

The proposed identification method enables a simultaneous computation of some significant BSPs in the human upper extremity. The experimental procedure is friendly from the subject point of view as it does not require any special fixation mechanisms and can be performed quickly.

The motivation for the presented study also comes as a result of new rehabilitation devices such as haptic robots (van de Hel et al., 2001), where this approach could enable an on-line parameter estimation technique used for evaluation purposes during rehabilitation practice. This would provide the physiotherapist with a new tool for evaluating the rehabilitation training progress by observing changes in body segment parameters (particularly joint passive

moments) on a daily basis. It is in such an application that we see the clinical use of the presented methodology. In developing the mathematical procedure the inspiration also came from mechanical segment identification techniques used on robotic manipulators (An et al., 1988; Siciliano and Sciavicco, 1996).

The accuracy of the method can be seen from results obtained on the mechanical arm experiment (Table 1 – upper part). The highest error rate of 10.6% can be observed for parameter τ_{p1R} which may appear relatively high. This figure originates mostly from a non-ideal mechanical model where the passive properties are not only brake produced, but arise also from a small amount of mechanical jitter and non-smooth point to point robot motion. These effects were observed from the load cell readings (not shown here) and manipulator-hand contact forces (Fig. 5 – left). Other errors can be attributed to similar reasons and are as high as 9.8% in l_{2R}. When observing this error we need to be well aware of the fact that it was obtained as $\frac{m_{2R}l_{2R}}{m_{2R}}$ and therefore includes errors in parameters $m_{2R}l_{2R}$ and m_{2R}. Besides, the error in $m_{2R}l_{2R}$ is also a consequence of error accumulation and also involves that of m_3 and τ_{p2}. (Eq. (7)) The same factor also explains higher errors in m_2l_2 and especially m_3l_3 in the human arm.

The human arm parameter errors were given in relation to literature estimates (Zatsiorsky and Seluyanov, 1983), which can not be viewed as an objective source since the errors there are of unpredictable nature. We speculate that the main reasons contributing to these errors are the rigid body the axial rotation and planar model simplifications which were made (Fig. 2). The other important error factor are inaccuracies in the measurement of joint angles and manipulator-hand contact forces (Fig. 5). While the former can be explained by an inaccurate marker fixation the later comes from a worse repeatability of human arm trajectories in comparison to the model. The errors in m_3l_3 and l_3 are relatively high for all three subjects, while the other parameters show more compliance to the literature. The reason for errors in the palm segment may be contributed to the fact that the wrist joint motion range was relatively small (around 1.8°). Passive moment references for the human subject were not given since they could not be reliably obtained.

It needs to be pointed out that we were well aware of the fact that the flexion extension movement of the upper extremity in the sagittal plane is not fully planar in reality. Nevertheless we think the results obtained in this study show that a planar simplification may yield results which are realistic.

When comparing this method to studies from the literature (Zatsiorsky and Seluyanov, 1983) a relatively good parameter comparability may be observed. Our aim in this paper was to show that an evaluation of some BSPs with the presented method is possible while a statistical analysis on a larger group of individuals remains the issue of future research. Despite the fact that the upper arm segment BSPs were only identified in a linear combination (m_1l_1) all obtained BSPs still undoubtedly represent subject specific data with obvious literature correlation (Zatsiorsky and Seluyanov, 1983).

By using the same method it would also be possible to perform an identification of segment moments of inertia as a second step of the identification procedure. In this case we would need to take the non-velocity and acceleration related terms obtained in this study and insert them into Eq. (1) by not discarding any terms. The trajectory under which the second identification step should be performed should then not be made under "quasi-static" conditions.

Apart from identifying upper extremity parameters the same methodology could also be useful on lower extremities or some other body segments.

We also believe that the proposed procedures will be of help in providing a number of higher accuracy personalized human locomotion system parameters in the fields of rehabilitation robotic systems and diagnostic procedures.

References

An, C., Atkeson, C., Hollerbach, J., 1988. Model-based Control of a Robot Manipulator. MIT Press.

Bernstein, N., 1947. On the construction of movements. Moscow, Medgiz (in Russian).

Clauser, C., McConville, J., Young, J., 1969. Technical Report AMRL-TR-69-70, Wright Patterson Air Force Base, Ohio.

de Leva, P., 1995. Journal of Biomechanics 29, 1223–1230.

Dempster, W., 1955. AMRL Technical Report – WrightPatterson Air Force Base, Ohio, 55–159.

Esteki, A., Mansour, J., 1996. Journal of Biomechanics 29, 443–450.

Harless, E., 1860. Treatises of the Math–Phys Class of the Royal Academy of Science of Bavaria 8, 69–96, 257–294 (in German).

Hatze, H., 1997. Clinical Biomechanics 12, 128–135.

Hinrichs, R., 1985. Journal of Biomechanics 18, 621–624.

Kodek, T., Munih, M., 2003. Journal of Technology and Health Care 11, 89–103.

Lawson, C., Hanson, R., 1974. Solving Least Squares Problems. Prentice-Hall.

Mansour, J., Audu, M., 1986. Journal of Biomechanics 5, 369–373.

Martin, P., Mungiole, M., Marzke, M., Longhill, J., 1989. Journal of Biomechanics 22, 367–376.

Mungiole, M., Martin, P., 1990. Journal of Biomechanics 23, 1039–1046.

Pataky, T., Zatsiorsky, V., Challis, J., 2003. Clinical Biomechanics 18, 364–368.

Reynolds, N., Walt, S., 2002. In: Proceedings of the 7th International Symposium on the 3-D Analysis of Human Movement. Newcastle, UK, pp. 76–79.

Riener, R., Edrich, T., 1999. Journal of Biomechanics 32, 539–544.

Siciliano, L., Sciavicco, B., 1996. Modeling and Control of Robot Manipulators. The McGraw-Hill Companies, Inc.

van de Hel, P., Diressen, B., Oderwald, M., Coote, S., Stokes, E., 2001. In: Proceedings of AAATE 2001, pp. 256–261.

Wei, C., Jensen, R., 1995. Journal of Biomechanics 28, 103–108.

Zatsiorsky, V., Seluyanov, V., 1983. International Biomechanics – Human Kinetic Illinois 4B, 1152–1159.